



Photodeoxygenation of phenanthro[4,5-*bcd*]thiophene *S*-oxide, triphenyleno[1,12-*bcd*]thiophene *S*-oxide and perylo[1,12-*bcd*]thiophene *S*-oxide

Satyanarayana M. Chintala, John T. Petroff II, Andrew Barnes & Ryan D. McCulla

To cite this article: Satyanarayana M. Chintala, John T. Petroff II, Andrew Barnes & Ryan D. McCulla (2019): Photodeoxygenation of phenanthro[4,5-*bcd*]thiophene *S*-oxide, triphenyleno[1,12-*bcd*]thiophene *S*-oxide and perylo[1,12-*bcd*]thiophene *S*-oxide, Journal of Sulfur Chemistry, DOI: [10.1080/17415993.2019.1615065](https://doi.org/10.1080/17415993.2019.1615065)

To link to this article: <https://doi.org/10.1080/17415993.2019.1615065>

 View supplementary material 

 Published online: 19 May 2019.

 Submit your article to this journal 

 Article views: 7

 View Crossmark data 



Photodeoxygenation of phenanthro[4,5-*bcd*]thiophene *S*-oxide, triphenyleno[1,12-*bcd*]thiophene *S*-oxide and perylo[1,12-*bcd*]thiophene *S*-oxide

Satyanarayana M. Chintala, John T. Petroff II, Andrew Barnes and Ryan D. McCulla

Department of Chemistry, Saint Louis University, St. Louis, MO, USA

ABSTRACT

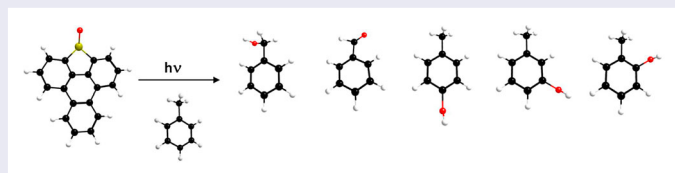
Sulfoxides, upon irradiation with ultraviolet (UV) light undergo α -cleavage, hydrogen abstraction, photodeoxygenation, bimolecular photoreduction, and stereo-mutation. The UV irradiation of dibenzothiophene *S*-oxide (DBTO) yields dibenzothiophene (DBT) as a major product along with ground-state atomic oxygen [$O(^3P)$]. This is a common method for generating $O(^3P)$ in solution. The low quantum yield of photodeoxygenation and the requirement of UVA light are drawbacks of using this method. The sulfoxides benzo[*b*]naphtho-[1,2-*d*]thiophene *S*-oxide, benzo[*b*]naphtho [2,1-*d*]thiophene *S*-oxide, benzo[*b*] phenanthro[9,10-*d*]thiophene *S*-oxide, dinaphtho- [2,1-*b*:1',2'-*d*]thiophene *S*-oxide, and dinaphtho[1, 2-*b*:2',1'-*d*]thiophene *S*-oxide have shown to deoxygenate up to three times faster than DBTO upon UVA irradiation; however, the photodeoxygenation of these sulfoxides does not appear to be limited to the production of $O(^3P)$. In this work, phenanthro[4,5-*bcd*]thiophene *S*-oxide, triphenyleno[1,12-*bcd*]thiophene-*S*-oxide, and perylo[1,12-*bcd*]thiophene-*S*-oxide were synthesized and their photodeoxygenation was studied. Phenanthro[4,5-*bcd*]thiophene-*S*-oxide, triphenyleno[1,12-*bcd*]thiophene-*S*-oxide, and perylo[1,12-*bcd*]thiophene-*S*-oxide deoxygenated upon UVA irradiation. However, the common intermediate experiments did not conclusively identify the photodeoxygenation mechanism of these sulfoxides.

ARTICLE HISTORY

Received 6 February 2019
Accepted 25 April 2019

KEYWORDS

Photodeoxygenation; sulfoxides; reactive oxygen species; triplet oxygen; toluene oxidation; 1-octene oxidation; polycyclic sulfoxide



1. Introduction

Ground-state atomic oxygen [$O(^3P)$] is a reactive oxidant which is selective towards certain functional groups such as thiols, alkenes, sulfides, and aromatics [1–10]. Photolysis of dibenzothiophene S-oxide (DBTO) upon irradiation with UVA light produces dibenzothiophene (DBT) and an oxidant purported to be ground-state atomic oxygen [4]. The chemical yield of formation of DBT from DBTO for this reaction is 95% [11]. However, the quantum yield of this reaction is very low at approximately 0.003 [4]. Photodeoxygenation of DBTO is a clean method of producing $O(^3P)$ in solution as it does not yield any by-products. Therefore, various derivatives of DBTO have been employed as $O(^3P)$ precursors to oxidize simple organic and biomolecules in condensed phase [3,5–7,12,13]. However, the requirement of high energy UVA light to induce the photodeoxygenation reaction combined with low photodeoxygenation quantum yield limits $O(^3P)$ from being utilized extensively as an oxidant in biological systems. Therefore, better precursors that absorb in the visible range and have a higher quantum yield of photodeoxygenation are desirable.

Photodeoxygenation of DBTO is believed to produce $O(^3P)$ in solution; however, there is no spectroscopic evidence to support it (Figure 1). $O(^3P)$ cannot be spectroscopically detected in solution due to the absence of an assessable spectroscopic signature. Therefore, $O(^3P)$ has been identified and characterized indirectly by its reactivity profile [1,2,4,6,10,14,15]. Recently more indirect evidence has been provided to show that oxidation reactions by photodeoxygenation of DBTO occur through freely diffusing $O(^3P)$ [16]. This has been done by the irradiation of a DBTO derivative inside of nanocapsules in the presence of an $O(^3P)$ accepting molecule outside the nanocapsules. The nanocapsules were not permeable to either the DBTO derivative or the $O(^3P)$ accepting molecule. The results showed that a small oxidant produced by photodeoxygenation, likely $O(^3P)$, diffused through the pores of the nanocapsules to oxidize the oxygen accepting molecule.

The most common technique to indirectly detect the generation of $O(^3P)$ in solution is the common intermediate experiment [4,10,12,14,17]. Common intermediate experiments are based on the principle that two different reactions may have a common intermediate if both reactions yield the same products in the same ratio. Hence, common intermediate experiments were used to test if the sulfoxides 1–5, shown in Figure 2, produce $O(^3P)$ by photodeoxygenation. These sulfoxides absorb near or into the visible region and have higher quantum yields of photodeoxygenation compared

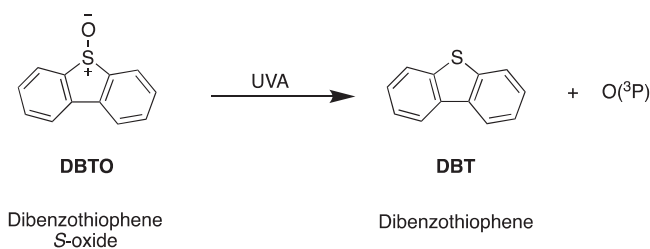


Figure 1. Photodeoxygenation of DBTO.

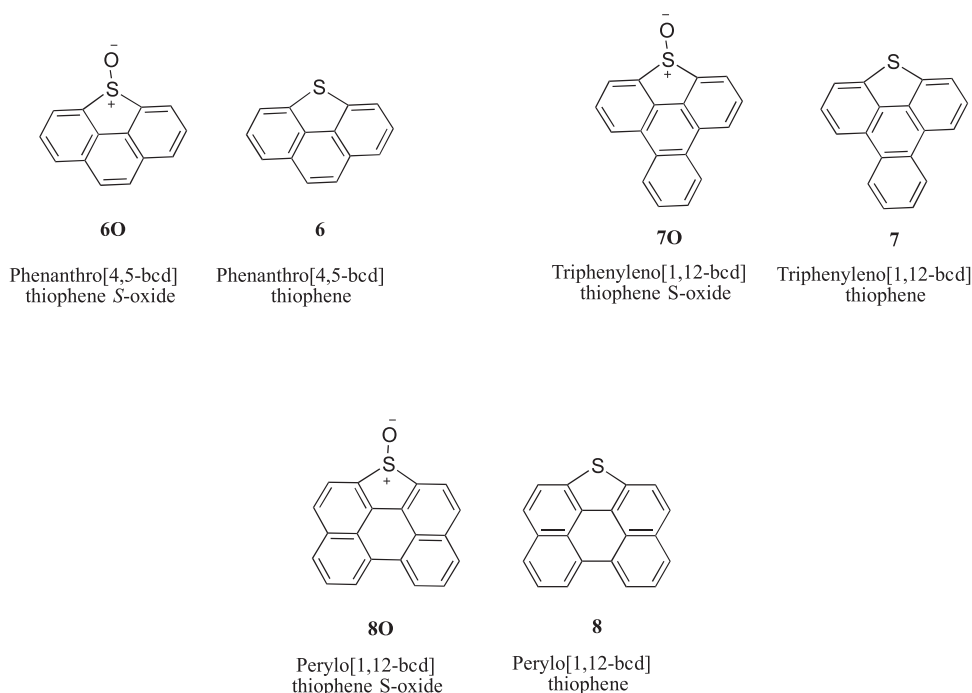


Figure 3. Sulfoxides and sulfides used in this study.

2. Experimental and computational methods

2.1. Materials

All commercially available materials were procured from Sigma Aldrich, Fisher Chemicals, or Oakwood Chemicals and are used directly without any purification except as mentioned. Anhydrous *N*-Methyl-2-pyrrolidone (NMP) obtained from Sigma Aldrich was further dried using 3 Å molecular sieves. Hexanes and tetramethylethylenediamine (TMEDA) were also dried using 3 Å molecular sieves. The concentration of *n*-butyllithium (*n*-BuLi) used was 1.6 M. HPLC grade toluene and acetonitrile were used for common intermediate experiments and determination of quantum yield of photodeoxygenation experiments.

2.2. General methods

The UV–Vis absorbance spectra for sulfoxides **6O–8O** were obtained using Shimadzu UV-1800 UV spectrophotometer. Shimadzu GC – 2010 plus was used to obtain the concentrations of products formed from the common intermediate experiments. An Agilent 1200 Series HPLC with a quaternary pump, diode-array detector and Higgins Analytical CLYPEUS C18 column (5 μm, 150 × 4.6 mm) was used for HPLC analysis. A Bruker DRX-400 NMR was used to obtain NMR spectra. The solvents CDCl₃ and deuterated dimethyl sulfoxide (DMSO-*d*₆) were used for obtaining NMR spectra. The chemical shift of CHCl₃ peak was set to 7.27 ppm and used as the reference peak for ¹H NMR performed in CDCl₃.

The chemical shift of dimethyl sulfoxide (DMSO) was set to 2.50 ppm for ^1H NMR spectra obtained in $\text{DMSO}-d_6$. Similarly, the chemical shift of CHCl_3 was set to 77.23 ppm for ^{13}C NMR obtained in CDCl_3 . The emission spectra of sulfoxide **8O** were obtained by using a Photon Technology International spectrofluorometer equipped with a 75 W Xenon arc steady state lamp, excitation monochromator, sample holder, emission monochromator and a PMT detector.

2.3. Common intermediate experiments

4 ml of saturated solutions of sulfoxides **6O–8O** were prepared and transferred into 5 ml quartz cuvettes (1 cm \times 1 cm). The solutions were prepared in toluene for the oxidation of toluene common intermediate experiment. For the oxidation of 1-octene common intermediate experiment, the sulfoxide solution was prepared in acetonitrile (ACN). The concentration of 1-octene in the prepared solution was 500 mM. The solutions were degassed by purging them by Argon. The degassed solutions were irradiated with Luzchem UVA bulbs (LZC – UVA), which are centered at 350 nm. For irradiation of sulfoxide **8O** with 420 nm light, Luzchem 420 nm bulbs (LZC-420) were used. Dodecane was used as the internal standard. The change in the sulfide concentration was measured using HPLC analysis. The concentrations of products formed were obtained using GC-FID analysis.

2.4. Determination of quantum yield of photodeoxygenation

Saturated solutions of sulfoxides **6O–8O** were prepared in acetonitrile. The solutions were transferred into quartz cuvettes (1 cm \times 1 cm) and degassed using Argon sparging. The degassed solutions were irradiated using 75 W Xenon lamp focus on a monochromator. The reactions were carried out to conversions lower than 20%. The increase in the sulfide concentration was measured by HPLC analysis. Photorearrangement of azoxybenzene to 2-hydroxyazobenzene was used as an actinometer [19].

2.5. Computational method

A comparative study has shown that HSEH1PBE method with 6-311G(d,p) basis set is a better method at predicting the vibrational frequencies of flufenpyr and amipizone more accurately compared to DFT/B3LYP and B3PW91 methods [20]. Therefore, HSEH1PBE method with 6-311G(d,p) basis set was used in this work. Initial guess geometries were generated by standard bond angles and lengths. The neutral species of DBTO, **6O**, **7O** and **8O** were analysed separately for molecular structure using HSEH1PBE methods with the 6-311G(d,p) basis set [20,21]. The geometry optimizations were performed with Gaussian 09 [22].

3. Results and discussion

3.1. Computed structures of compounds **6O–8O**

The computed structures for sulfoxides **6O–8O** are shown in Figure 4. These structures were obtained by HSEH1PBE/6-311G(d,p) geometry optimizations with Gaussian09 [20,21]. The optimized structures of sulfoxides DBTO, **6O–8O** were planar and the

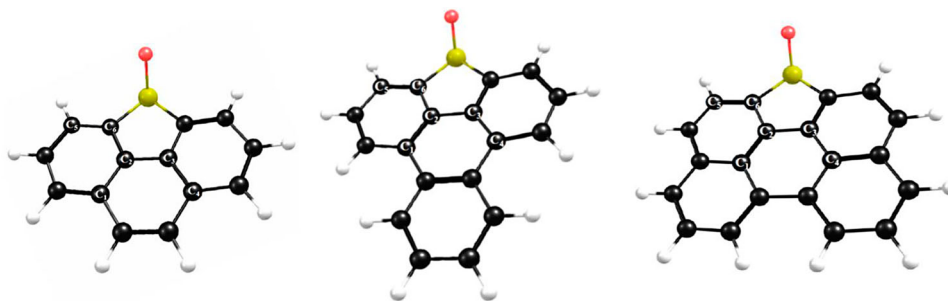


Figure 4. Computed Structures of Sulfoxides **60–80**.

Table 1. Dihedral Angles of Sulfoxides **60–80**.

Sulfoxide	C ₁ –C ₂ –C ₃ –C ₄ Dihedral Angle	C ₅ –C ₆ –S–O Dihedral angle
DBTO	0.006°	62.0°
60	0.005°	63.8°
70	0.003°	63.1°
80	0.001°	63.0°

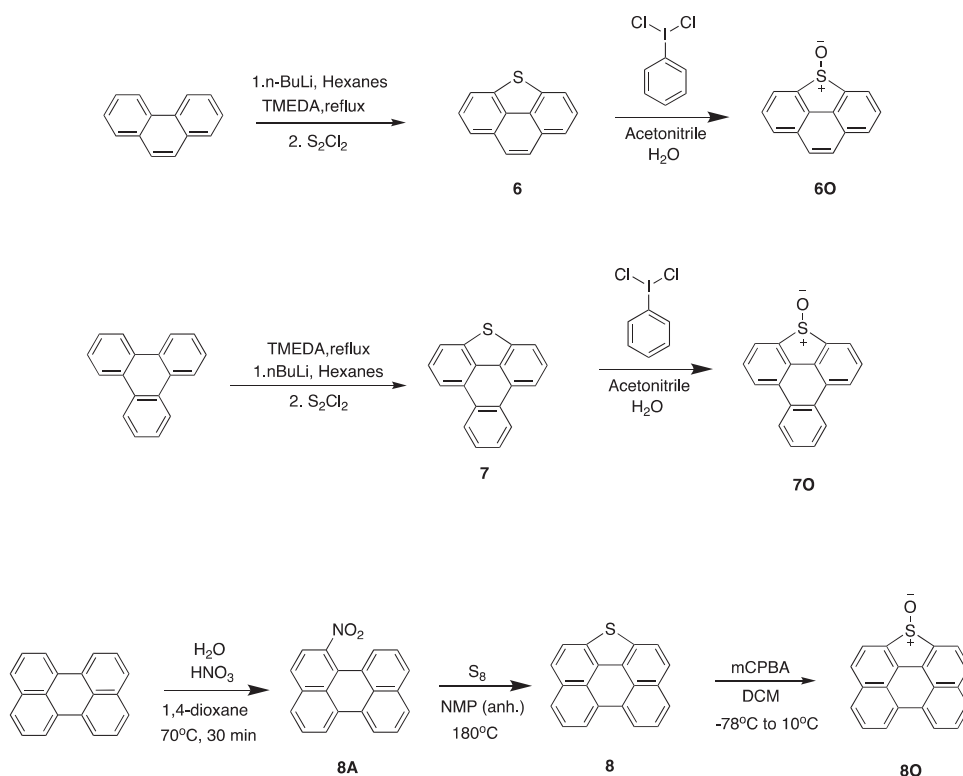
dihedral angles C₁–C₂–C₃–C₄ and C₅–C₆–S–O of sulfoxides DBTO, and **60–80** are shown in Table 1. The dihedral angle C₅–C₆–S–O was used to show the angle created by the S–O bond and the plane of the aromatic system. No significant differences were observed. The calculations of structural geometry optimization, zero-point correction, thermal correction to energy, thermal correction to enthalpy, and thermal correction to Gibbs free energy are provided in the supporting information.

3.2. Synthesis of compounds **60–80**

Compounds dichloro iodobenzene, **60**, **70**, **7** and **8** were synthesized according to the reported procedures [23–28]. Compounds **60** and **70** have similar synthetic procedures which are shown in Scheme 1 [23]. The first step of their syntheses involves refluxing of the polycyclic aromatic hydrocarbon with *n*-BuLi in the presence of TMEDA followed by addition of S₂Cl₂ at 0°C. The next step is the oxidation of sulfide to sulfoxide by dichloro iodobenzene and water in acetonitrile. Compound **8** was prepared in two steps [24]. The first step was nitration of perylene using nitric acid in a dioxane/water solvent mixture which gave 1-nitroperylene (**8A**). The second step involved heating of **8A** in the presence of sulfur to yield **8**. Sulfoxide **80** was obtained by oxidation of **8** using *meta*-chloroperbenzoic acid (mCPBA) as shown in Scheme 1. The temperature of the reaction was maintained under 5°C to reduce the formation of the sulfone by-product. The detailed synthetic procedures of dichloro iodobenzene, **6–8** and **60–80** are provided in the supporting information.

3.3. UV-Vis spectra of sulfoxides **60–80**

Photodeoxygenation of DBTO requires irradiation of UVA light as the UV-Vis absorption of DBTO does not extend past 350 nm [14]. This is one of the drawbacks of utilizing



Scheme 1. Synthesis of sulfoxides **60–80**. *N*-Methyl-2-pyrrolidone (NMP), 3-chloroperbenzoic acid (mCPBA), tetramethylethylenediamine (TMEDA).

photodeoxygenation of DBTO for generation of $O(^3P)$ in biological systems. The UV-Vis spectra of sulfoxides **60–80** were obtained to determine if the absorption extends past into visible wavelength range. The UV-Vis spectra of **60–80** are shown in Figure 5. The UV-Vis cut-off wavelengths ($\epsilon < 100 \text{ M}^{-1} \text{ cm}^{-1}$) for **60–80** are 364, 358, and 566 nm respectively. Only sulfoxide **80** had UV-Vis absorption spectra which extended into the visible wavelength range. In addition, sulfoxide **80** has two luminescence peaks at 437 and 414 nm when excited using 380 nm light. The emission spectrum of **80** is provided in the supporting information.

3.4. Quantum yield of photodeoxygenation of **60–80**

The quantum yield of photodeoxygenation of DBTO is wavelength dependent and is approximately 0.003 at 320 nm in ACN [4]. The sulfoxides shown in Figure 2 have up to three times higher quantum yield of photodeoxygenation compared to DBTO. The quantum yields of photodeoxygenation of **60–80** were measured based on the increase in the corresponding sulfide concentration. The quantum yields of photodeoxygenation of **60–80** are listed in Table 2. For photolysis of **60–80**, the wavelength with the highest extinction coefficient above 320 nm in their corresponding UV-Vis spectrum was used as the irradiation wavelength.

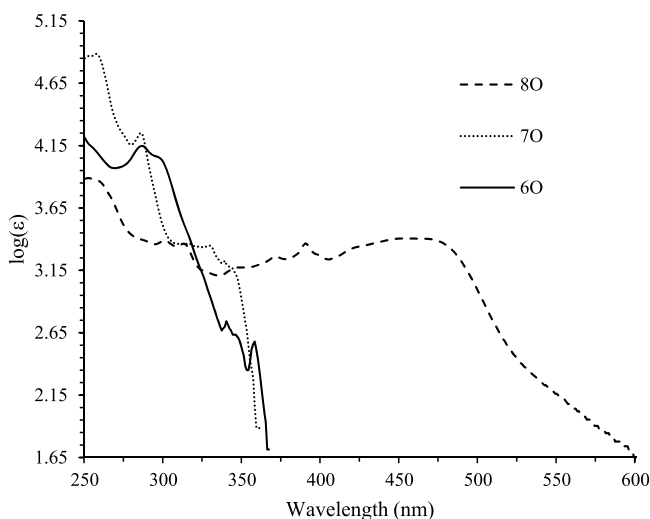


Figure 5. UV-Vis spectra of **60–80**.

Table 2. Quantum yields of photodeoxygenation of compounds DBTO and **60–80**.

Compound	Quantum yield ^b $\Phi_{+\text{sulfide}}$	Wavelength (nm)
DBTO ^a	0.0026 ± 0.0004	320 ± 12
60	0.0007 ± 0.0003	320 ± 6
70	0.0028 ± 0.0001	329 ± 6
80	0.00010 ± 0.00001	320 ± 6

^aQuantum yield of photodeoxygenation of DBTO from Ref. [4].

^bQuantum yields reported are within 95% confidence intervals and were calculated by increase in sulfide concentration.

Photodeoxygenation of **60–80** yielded their corresponding sulfides. No other significant products were obtained in HPLC analysis. The quantum yields of photodeoxygenation of sulfoxides **60–80** ranged from 0.0001–0.0028. The values of quantum yield of photodeoxygenation of sulfoxides **60** and **80** are 0.0007 ± 0.0003 and 0.00010 ± 0.00001 respectively. These values are lower than the quantum yield of photodeoxygenation of DBTO. The quantum yield of photodeoxygenation of **70** was 0.0028 ± 0.0001 , which was in the range of the quantum yield of photodeoxygenation of DBTO.

3.5. Oxidation of toluene as a common intermediate experiment

The oxidation of toluene has been previously used to verify whether aryl sulfoxides produce $O(^3P)$ on photodeoxygenation [4,9,12,14]. As shown in Figure 6, oxidation of toluene by photodeoxygenation of DBTO yields benzaldehyde, benzyl alcohol, *o*-cresol, *m*-cresol, and *p*-cresol. These products are always obtained in a certain product ratio as shown in Table 3. Therefore, if the oxidation of toluene by photodeoxygenation of a sulfoxide yields benzaldehyde, benzyl alcohol, *o*-cresol, *m*-cresol and *p*-cresol in the same ratio as in the case of DBTO then the sulfoxide and DBTO likely have a common intermediate of photodeoxygenation. Toluene was oxidized by photodeoxygenation of sulfoxides **60–80** by

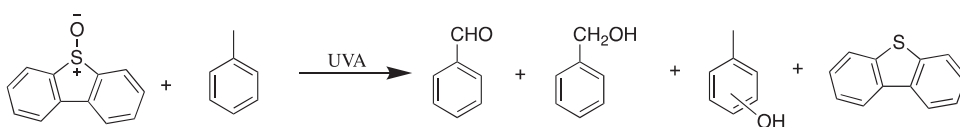


Figure 6. Oxidation of toluene by photodeoxygenation of DBTO.

Table 3. Product distribution and yields of toluene oxidation by photolysis of DBTO and **60–80**.

Compound	Percentage product yield (%) ^a				Total product yield (%)	CH ₃ :Ring ^c
	Benzaldehyde	Benzyl alcohol	<i>o</i> -Cresol	<i>m/p</i> -Cresol ^b		
DBTO	5 ± 3	6 ± 3	17.6 ± 0.9	13 ± 1	42 ± 6	1:3
60	2 ± 1	3 ± 1	14 ± 1	7 ± 1	26 ± 4	1:4
70	2 ± 1	3 ± 1	7 ± 1	3 ± 1	15 ± 4	1:2
80	5 ± 1	4 ± 1	12.9 ± 0.1	5.6 ± 0.2	28 ± 2	1:2

^aPercentage product yields are calculated with respect to formation of sulfide and are within 95% CI.

^bCalculated as one peak.

^cRatio of sum of yields of PhCHO and benzyl alcohol to combined yields of cresols.

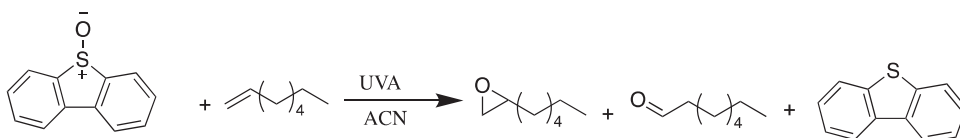


Figure 7. Oxidation of 1-octene by photodeoxygenation of DBTO.

irradiation with UVA light. The oxidized toluene product ratios and total product yields were then obtained. The details of the common intermediate test are shown in Table 3.

Sulfoxides **60–80** oxidized toluene to benzaldehyde, benzyl alcohol, *o*-cresol, *m*-cresol and *p*-cresol. The ratios of CH₃:ring oxidation obtained for DBTO and **60–80** were 1:3, 1:4, 1:2 and 1:2, respectively. Although the ratios of CH₃:ring oxidation obtained for **60–80** are similar to the CH₃:ring oxidation ratio obtained for DBTO, the total product yields of **60–80** were lower to that of DBTO. The total product yields of toluene oxidation obtained for DBTO and **60–80** were 42 ± 6%, 27 ± 2%, 15 ± 4%, and 28 ± 2%, respectively. This is because the yields of cresols (ring oxidation) obtained for **60–80** were lower compared to DBTO. The ratios of the oxidized products obtained for **60–80** suggests O(³P) formation. However, the lower total product yields suggest other photodeoxygenation pathways that do not generate O(³P).

3.6. Oxidation of 1-octene common intermediate experiment

As the oxidation of toluene common intermediate experiment indicated that **60–80** may produce O(³P) with lower product yields, and thus, the oxidation of 1-octene was performed to determine if the total product yields of **60–80** would be lower as well. O(³P) reacts with 1-octene to yield 1-octanal and 1,2-epoxyoctane as shown in Figure 7 [2]. To confirm that O(³P) was the intermediate formed during the photodeoxygenation process, 1-octene was oxidized by photodeoxygenation of sulfoxides **60–80** in acetonitrile. The details are shown in Table 4.

Table 4. Product distribution and yields of 1-octene oxidation by photolysis of DBTO and **6O–8O**.

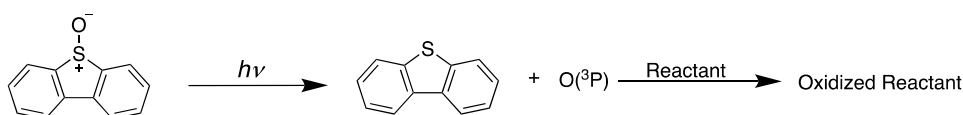
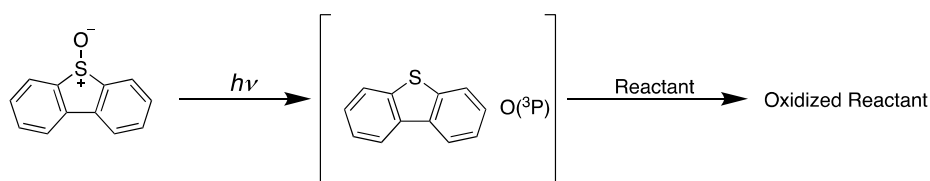
Compound	Product yields ^a		Total product yield (%)	Aldehyde: epoxide ^b
	1-octanal (%)	1,2-epoxyoctane (%)		
DBTO	24 ± 2	35 ± 3	59 ± 6	1: 1.4
6O	8.6 ± 0.6	1.7 ± 0.1	10.3 ± 0.7	5.1: 1
7O	4.4 ± 1.1	2.0 ± 1.0	6.4 ± 2.1	2.2: 1
8O	Not detected	Not detected	–	–

^aPercentage product yields are calculated with respect to formation of sulfide and are within 95% CI.

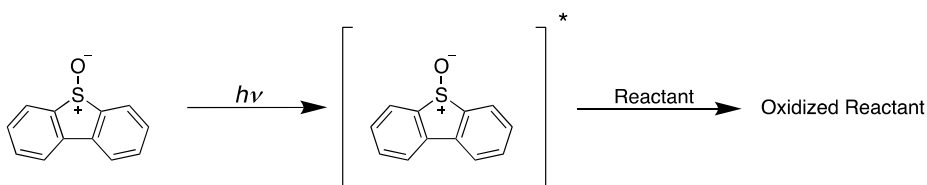
^bRatio of yield of 1-octanal to yield of 1,2-epoxyoctane.

Sulfoxides **6O** and **7O** along with DBTO upon UVA irradiation oxidized 1-octene to 1-octanal and 1,2-epoxyoctane. However, the ratio of 1-octanal:1,2-epoxyoctane obtained for **6O**, **7O** were very different than the ratio obtained for DBTO. The ratio of 1-octanal:1,2-epoxyoctane obtained for DBTO was 1:1.4 with the total product yield of 59 ± 6%. Sulfoxide **6O** yielded 1-octanal and 1,2-epoxyoctane in the ratio of 5.1:1 with total product yield of 10.3 ± 0.7%. Sulfoxide **6O** yielded more 1-octanal compared to 1,2-epoxyoctane, and the total product yield obtained for **6O** was lower than that of DBTO. Sulfoxide **7O** showed a 1-octene oxidation pattern similar to **6O**. Sulfoxide **7O** on reaction with 1-octene yielded more 1-octanal compared to 1,2-epoxyoctane. The ratio of 1-octanal: 1,2-epoxyoctane was 2.1:1. Like **6O**, the total product yield obtained for **7O**, 6.4 ± 2.1%, was significantly lower to DBTO. Sulfoxide **8O** did not yield any observable 1-octene oxidation products. As the absorption spectrum of sulfoxide **8O** extends into the visible wavelength range, oxidation of 1-octene common intermediate experiment was performed by irradiation of **8O** by 420 nm light. This resulted in photodeoxygenation of **8O** to **8**; however, no 1-octene oxidation products were observed in the GC-FID analysis.

Photodeoxygenation of DBTO occurs through a unimolecular scission of S–O bond in pure acetonitrile [4]. However, in an aqueous medium, the mechanism of photodeoxygenation of DBTO is dependent on the pH of the solution [15]. At neutral and acidic pH, photodeoxygenation of DBTO has been suspected to have the unimolecular scission mechanism. In basic pH, DBTO photodeoxygenates through a bimolecular photoinduced electron transfer mechanism. As the common intermediate experiments of **6O–8O** was performed in acetonitrile, we considered all the unimolecular mechanisms of oxidation that have been considered for DBTO photodeoxygenation to rationalize the results of the common intermediate experiments of **6O–8O**. In previous studies, three different pathways of oxidation of a reactant by the photodeoxygenation of DBTO has been suggested as shown in Scheme 2 [2,4,16]. The first mechanism is the release of a freely diffusing O(³P) into the bulk solution, which has been recently supported with evidence that the oxidant can pass through a nanocapsule barrier that prevents the diffusion of the sulfoxide [16]. In addition to freely diffusing O(³P), the oxidation of the reactant can occur before the oxidant escapes the solvent cage (Scheme 2(a)) [2]. Oxidation prior to escape from the solvent cage has been suggested to occur by two different mechanisms. One possibility is the formation of discrete O(³P) that reacts with a reactant molecule prior to escape from the solvent cage (Scheme 2(b)). A second possibility is an oxygen-atom transfer from an excited state DBTO directly to the reactant (Scheme 2(c)). While the previous experiments were unable to distinguish between 2b and 2c for DBTO, the ratio of oxidation products

a) Freely diffusing O(³P)b) Solvent caged discrete O(³P)

c) O-atom transfer



Scheme 2. Different pathways of oxidation by DBTO photodeoxygenation.

produced by either 2b or 2c would have to be the same as freely diffusing $O(^1P)$ (2a) to conform with the experimental results.

Unfortunately, the data obtained from the common intermediate experiments do not conclusively identify the photodeoxygenation mechanisms of **6O–8O**. The oxidation of toluene by photodeoxygenation of **6O–8O** in neat toluene yielded similar product ratios and slightly lower product yields compared to DBTO. In contrast, the oxidation of 1-octene dissolved in acetonitrile by photodeoxygenation of **6O–8O** resulted in different product ratios and significantly lower product yields compared to DBTO. In toluene, the lower yields obtained for **6O–8O** compared to DBTO could be explained if **6O–8O** deoxygenates by an additional mechanism that does not produce $O(^1P)$. However, the very low yields and the different products observed for 1-octene are inconsistent with **6O–8O** generating $O(^1P)$ in acetonitrile.

One possible reason for this difference is if **6O–8O** undergo photodeoxygenation by a different mechanism than DBTO. For example, if **6O–8O** undergo photodeoxygenation by an oxygen-atom transfer similar to Scheme 2(c), it is plausible that the observed oxidized products would be different than $O(^1P)$ generated by DBTO. However, this would require

the oxygen-atom transfer mechanism of **6O–8O** to give the same ratio of oxidized products as $O(^3P)$ in toluene. Another potential rationale for this difference is the mechanism of photodeoxygenation for **6O–8O** is different in toluene than acetonitrile. For example, the observed products could arise if **6O–8O** generated $O(^3P)$ in toluene but not in acetonitrile. However, it seems somewhat unlikely that a modest change in solvent would result in such a significant change in the mechanism.

4. Conclusion

The photodeoxygenation process of sulfoxides **6O–8O** was investigated and the nature of the oxidant produced during this process was studied. The common intermediate experiments did not conclusively identify the oxidant generated during the photodeoxygenation of **6O–8O**. This oxidant produced during photodeoxygenation of **6O–8O** oxidized toluene to cresols, benzyl alcohol, and benzaldehyde. Similarly, oxidation of 1-octene yielded 1-octanal and 1,2-epoxyoctane. Additionally, the product yields of the common intermediate experiments of **6O–8O** were lower compared to DBTO. While the quantum yield of photodeoxygenation of **7O** was in the range of DBTO, sulfoxides **6O** and **8O** had lower quantum yields of photodeoxygenation compared to DBTO.

Funding

This work was supported by grants CHE-1255270 from the National Science Foundation and donors to the Herman Frasch Foundation for Chemical Research.

Disclosure statement

No potential conflict of interest was reported by the authors.

References

- [1] Bucher G, Scaiano JC. Laser flash photolysis of pyridine N-oxide: kinetic studies of atomic oxygen [$O(^3P)$] in solution. *J Phys Chem.* **1994**;98:12411–12413.
- [2] Omlid SM, Zhang M, Isor A, et al. Thiol reactivity toward atomic oxygen generated during the photodeoxygenation of dibenzothiophene S-oxide. *J Org Chem.* **2017**;82:13333–13341.
- [3] Zhang M, Ravilious GE, Hicks LM, et al. Redox switching of adenosine-5'-phosphosulfate kinase with photoactivatable atomic oxygen precursors. *J Am Chem Soc.* **2012**;134:16979–16982.
- [4] Gregory DD, Wan Z, Jenks WS. Photodeoxygenation of dibenzothiophene sulfoxide: evidence for a unimolecular S-O cleavage mechanism. *J Am Chem Soc.* **1997**;119:94–102.
- [5] Wauchope OR, Shakya S, Sawwan N, et al. Photocleavage of plasmid DNA by dibenzothiophene S-oxide under anaerobic conditions. *J Sulfur Chem.* **2007**;28:11–16.
- [6] Thomas KB, Greer A. Gauging the significance of atomic oxygen [$O(^3P)$] in sulfoxide photochemistry. A method for hydrocarbon oxidation. *J Org Chem.* **2003**;68:1886–1891.
- [7] Korang J, Emahi I, Grither WR, et al. Photoinduced DNA cleavage by atomic oxygen precursors in aqueous solutions. *RSC Adv.* **2013**;3:12390.
- [8] Bourdillon MT, Ford BA, Knulty AT, et al. Oxidation of plasmalogen, low-density lipoprotein and raw 264.7 cells by photoactivatable atomic oxygen precursors. *Photochem Photobiol.* **2014**;90:386–393.
- [9] McCulla RD, Jenks WS. Deoxygenation and other photochemical reactions of aromatic selenoxides. *J Am Chem Soc.* **2004**;126:16058–16065.

- [10] Rockafellow EM, McCulla RD, Jenks WS. Deoxygenation of dibenzothiophene-S-oxide and dibenzoselenophene-Se-oxide: a comparison of direct and sensitized photolysis. *J Photochem Photobiol A Chem.* **2008**;198:45–51.
- [11] Gurria GM, Posner GH. Photochemical deoxygenation of aryl sulfoxides. *J Org Chem.* **1973**;38:2419–2420.
- [12] Petroff JT, Omlid SM, Chintala SM, et al. Wavelength dependent photochemistry of expanded chromophore and asymmetric dibenzothiophene S-oxide derivatives. *J Photochem Photobiol A Chem.* **2018**;358:130–137.
- [13] Omlid SM, Isor A, Sulkowski KL, et al. Synthesis of aromatic disulfonic acids for water-soluble dibenzothiophene derivatives. *Synthesis.* **2018**;50:2359–2366.
- [14] Zheng X, Baumann SM, Chintala SM, et al. Photodeoxygenation of dinaphthothiophene, benzophenanthrothiophene, and benzonaphthothiophene S-oxides. *Photochem Photobiol Sci.* **2016**;15(6):791–800.
- [15] Korang J, Grither WR, Mcculla RD. Photodeoxygenation of dibenzothiophene S-oxide derivatives in aqueous Media. *J Am Chem Soc.* **2010**;132:4466–4476.
- [16] Omlid SM, Dergunov SA, Isor A, et al. Evidence for diffusing atomic oxygen uncovered by separating reactants with a semi-permeable nanocapsule barrier. *Chem Commun.* **2019**;55(12):1706–1709.
- [17] Lucien E, Greer A. Electrophilic oxidant produced in the photodeoxygenation of 1,2-benzodiphenylene sulfoxide. *J Org Chem.* **2001**;66:4576–4579.
- [18] Stoffregen SA, Lee SY, Dickerson P, et al. Computational investigation of the photochemical deoxygenation of thiophene-S-oxide and selenophene-Se-oxide. *Photochem Photobiol Sci.* **2014**;13:431–438.
- [19] Bunce NJ, Lamarre J, Vaish SP. Photorearrangement of azoxybenzene to 2-hydroxyazobenzene: a convenient chemical actinometer*. *Photochem Photobiol.* **1984**;39:531–533.
- [20] Avcı D, Bahçeli S, Tamer Ö, et al. Comparative study of DFT/B3LYP, B3PW91, and HSEH1PBE methods applied to molecular structures and spectroscopic and electronic properties of flufenpyr and amipizone. *Can J Chem.* **2015**;93:1147–1156.
- [21] Avcı D, Altürk S, Sönmez F, et al. Three novel Cu(II), Cd(II) and Cr(III) complexes of 6-methylpyridine-2-carboxylic acid with thiocyanate: Synthesis, crystal structures, DFT calculations, molecular docking and α -Glucosidase inhibition studies. *Tetrahedron.* **2018**;74:7198–7208.
- [22] Frisch MJ, Trucks GW, Schlegel HB, et al. Gaussian 09, Revision E.01. Wallingford (CT): Gaussian, Inc; **2009**.
- [23] Ashe AJ, Kampf JW, Savla PM. Selective functionalization in the bay region of polycyclic aromatic hydrocarbons via dilithiation. *J Org Chem.* **1990**;55:5558–5559.
- [24] Jiang W, Qian H, Li Y, et al. Heteroatom-annulated perylenes: practical synthesis, photophysical properties, and solid-state packing arrangement. *J Org Chem.* **2008**;73:7369–7372.
- [25] Carle MS, Shimokura GK, Murphy GK. Iodobenzene dichloride in the esterification and amidation of carboxylic acids: in-situ synthesis of Ph₃PCl₂. *Eur J Org Chem.* **2016**;2016:3930–3933.
- [26] Klemm LH, Mccoy DR, Olson DR. Condensed thiophenes from sulfur bridging. I. Phenanthro[4,5-bcd]thiophene. *J Heterocycl Chem.* **1970**;7:1347–1352.
- [27] Klemm LH, Lawrence RF. The insertion and extrusion of heterosulfur bridges. X. Conversions in the triphenylene-triphenylo[4,5-bcd] thiophene system. *J Heterocycl Chem.* **1979**;16:599–601.
- [28] Powers DC, Ritter T. Bimetallic Pd(III) complexes in palladium-catalysed carbon-heteroatom bond formation. *Nat Chem.* **2009**;1:302–309.